

Evolution of volatility and composition in sesquiterpene-mixed and α -pinene secondary organic aerosol particles during isothermal evaporation

- 5 Zijun Li¹, Angela Buchholz¹, Arttu Ylisirniö¹, Luis Barreira^{1,2}, Liqing Hao¹, Siegfried Schobesberger¹, Taina Yli-Juuti¹, Annele Virtanen^{1,*}

¹Department of Applied Physics, University of Eastern Finland, Kuopio, Finland

²Atmospheric Composition Research, Finnish Meteorological Institute, Helsinki, Finland

Correspondence to: Annele Virtanen (annele.virtanen@uef.fi)

Supplement material

S1.1 Experimental approach for isothermal evaporation of secondary organic aerosol (SOA) particles

15 The experimental sequence consisted of SOA production, particle size selection, humidity-controlled SOA particle evaporation, and particle characterization. The schematic diagram of experimental setup is shown in Figure S1, and the experimental conditions and results are summarized in Table S1.

S1.1.1 SOA Production

20 SOA was generated by oxidizing two different types of BVOCs in a 13 L oxidation flow reactor (OFR, Aerodyne Research Inc.) (Kang et al., 2007; Lambe et al., 2011). Either α -pinene (Sigma-Aldrich, 98%) or a sesquiterpene mixture (Sigma-Aldrich, mixture of isomers) which consists of farnesenes and bisabolenes was used for generating SOA. A syringe pump system (Kari et al., 2018) was used to constantly inject liquid VOC precursors into 1.3 L min⁻¹ of heated N₂ flow. Before entering the OFR, the VOC-containing flow was mixed with a humidified flow of N₂ and O₃. To achieve the target RH, water vapor was introduced by passing 5.3 L min⁻¹ of N₂ through a Nafion humidifier (Model FC 100-80-6MSS, Perma Pure). O₃ was generated externally by passing 0.45 L min⁻¹ of O₂ via an ozone generator with a 185-nm UV lamp. Prior to mixing with O₃, the concentration of VOC was continuously monitored by a proton transfer reaction time-of-flight mass spectrometer (PTR-TOF 8000, Ionicon Analytik) using H₃O⁺ reagent ions. Eventually, 5.3 L min⁻¹ of total flow containing VOC (254 – 261 ppb) and O₃ (13.01 – 13.40 ppm) with RH of 41% - 44% was introduced into the OFR for photooxidation at controlled temperature (~ 25 °C), with 160 sec residence time inside the OFR.

30 Under the illumination of 254-nm lamps, O(¹D) was generated from the photolysis of O₃ and consecutively reacted with H₂O to produce OH radicals. We produced the α -pinene (α pin) and the sesquiterpene mixture (SQTmix) SOA under comparable oxidation conditions. According to the OFR model (Peng et al., 2015; Peng et al., 2016) which accounts for the external OH activity, the OH exposure was between 0.9 and 2.6×10¹¹ molec cm⁻³, equivalent to 0.7 to 2 days of atmospheric aging. Before each SOA experiment, we conducted photochemical cleaning of the OFR overnight (~ 8 hr.) by flushing the OFR with purified air at the desired concentration of OH but without adding any VOC. After an overnight photochemical cleaning, the background particle number was below 2000 # cm⁻³ (particle mass < 0.1 μ g m⁻³) and VOC concentration was below the instrument limit of detection.

35 S1.1.2 Particle Size Selection

Following the SOA generation in the OFR, 2 L min⁻¹ of sample flow was passed through an ozone denuder coated with potassium iodide. Two parallel nano differential mobility analyzers (NanoDMA, model 3085, TSI) were then employed to select a narrow distribution of SOA particles with a mobility equivalent diameter of 80 nm, and simultaneously dilute the surround gas phase by two orders of magnitude, which initiates isothermal evaporation at the outlet of the NanoDMAs. To remove the majority of gas vapors, each NanoDMA was operated with an open loop sheath flow at a sample-to-sheath flow ratio of 1:8 or 1:10. To control the RH of the samples, we humidified/dried the sheath flow of the NanoDMAs by mixing a dry and a humidified air flow.

S1.1.3 Humidity-Controlled Particle Evaporation

After exiting the NanoDMAs, the monodisperse particle sample was fed (i) to bypass lines with varying lengths for short residence time measurements of up to 3 min, (ii) to a 25 L stainless-steel residence time chambers (RTC) for intermediate measurements

45 with 10 min intervals for up to 40 min, and (iii) to a 100 L RTC for long measurements with 1 h intervals for up to 7.5 h. We initiated the RTC experiments by filling the RTC with monodisperse particle sample for 5 min (25 L RTC) or 20 min (100 L RTC). After the particle filling, we immediately sealed the RTC. Periodically, the RTC was opened for sampling. At the same time, purified air with the same RH was supplied into the RTC to compensate for the removed air volume to maintain constant pressure and humidity, which resulted in a dilution factor below 1.2. For each SOA type, evaporation experiments were conducted under
50 one of three desired RH conditions (i.e., dry (< 7% RH), intermediate (40% RH), or high (80% RH)). Once each evaporation experiment was completed, we flushed the NanoDMAs, bypass lines, and RTCs with purified air at the desired RH of the following experiment for at least 12 h.

S1.1.4 Particle Characterization

The size changes of monodisperse SOA particles due to isothermal evaporation were measured by a scanning mobility particle
55 sizer (SMPS, model 3080, TSI). Since we only rely on the particle size to evaluate the extent of particle evaporation, any decrease in the particle number or mass concentration (due to, e.g., wall losses or dilution) only limits the number of times for particle sampling from the RTC. The selected particle size was calibrated against dry ammonium sulfate particles. The volume fraction remaining (VFR) was calculated as the cubic ratio of the particle size ($D_{p,t}$) measured after time t of evaporation and the selected size ($D_{p,0}$) at the start of evaporation as follows:

$$60 \quad VFR = \left(\frac{D_{p,t}}{D_{p,0}}\right)^3 \quad (\text{S1, Eq. 1 in main text})$$

The elemental composition of the particle sample was determined using a high-resolution time-of-flight aerosol mass spectrometer (HR-ToF-AMS, Aerodyne Research Inc.) and was analyzed using the TOF-AMS toolkits (SQUIRREL 1.59C and PIKA 1.19C). We determined the oxidation state (OSc = 2O:C – H:C) of monodisperse particle samples exiting the NanoDMAs with the improved ambient parameterizations (Canagaratna et al., 2015). As the particle concentration after the RTC evaporation was too
65 low for reliable elemental composition measurements, we only present the compositional data from the bypass tubing measurements which exhibited the least amount of isothermal evaporation.

The thermal desorption behavior and chemical composition of particle samples were characterized using a custom-built Filter Inlet for Gases and AEROsols (FIGAERO) (Ylisirnio et al., 2021) in combination with a chemical ionization mass spectrometer (CIMS, Aerodyne Research Inc.) using iodide as reagent ion (Lopez-Hilfiker et al., 2014). The mass resolution CIMS was ranging from
70 4000 to 5000 and the pressure of the ion molecule reaction (IMR) chamber was constantly maintained at 100 mbar. Each particle sample after size selection (i.e., fresh samples) or isothermal evaporation in the RTC (i.e., RTC samples) was collected for analysis on a PTFE filter (2 μm pore, Zefluor, Pall Corp.) for 30 min in the FIGAERO. After sample collection, the collected particles were desorbed with a N_2 flow of which the temperature was linearly increased from 25 $^\circ\text{C}$ to ~ 190 $^\circ\text{C}$ in 20 min (desorption period) and maintained at above 190 $^\circ\text{C}$ for additional 15 min (soak period). The relationship between the temperature of maximum desorption
75 signal (T_{max}) of a single compound and its saturation vapor pressure (C^*) was calibrated by measuring polyethylene glycol (PEG, PEG 4 - 8) particles with known vapor pressures (Ylisirnio et al., 2021).

The analysis of the raw FIGAERO-CIMS data was performed using Tofware (version 3.2, TOFWERK AG). Prior to fitting the high-resolution mass spectra data, the data were averaged over 10 sec of measurement time and a baseline correction was applied. The filter blank samples were analyzed in the same manner as the particle samples. To identify instrument background and
80 contamination from the surrounding gas, we performed two types of blank measurements: (i) Measurements of the clean FIGAERO filter without collecting particles for characterizing the overall instrument background. (ii) Measurements of filter sampled after

size selection for 30 min but with the NanoDMAs voltage set to 0V for characterizing the background due to adsorption of gas-phase compounds during the time of normal sample collection.

S1.2 Analysis of FIGAERO-CIMS data using positive matrix factorization (PMF)

85 S1.2.1 General method and selection of error scheme

The PMF model expresses the measured mass spectra matrix \mathbf{X} by a combination of a number, p , of constant factors with varying concentrations with time (Paatero and Tapper, 1994; Ulbrich et al., 2009):

$$\mathbf{X} = \mathbf{GF} + \mathbf{E} \quad (\text{S2})$$

\mathbf{X} is a $m \times n$ matrix containing the measured mass spectra, with m rows of mass spectra averaged over 10 sec of measurement time and n columns containing the time series of one specific ion. \mathbf{G} is a $m \times p$ matrix containing the factor time series as columns. The rows of the $p \times n$ matrix \mathbf{F} contain the factor mass spectra. Then the $m \times n$ matrix \mathbf{E} contains the residuals between the measured data and the fitted values. To account for uncertainties in the measurement data, the PMF model weights the data points with their measurement error (S_{ij}). Values for \mathbf{G} and \mathbf{F} are constrained to be positive and iteratively found by minimizing the quantity (Q) with a least square algorithm (Paatero and Tapper, 1994):

$$95 \quad Q = \sum_{j=1}^m \sum_{i=1}^n \left(\frac{E_{ij}}{S_{ij}} \right)^2 \quad (\text{S3})$$

S_{ij} is the error (uncertainty) of each measurement data point. In an ideal case, the Q value of the model should approach the expected Q value ($Q_{exp} \approx n \cdot m$) which is equal to the degree of freedom of the model solution.

The chosen measurement error values have a direct impact on the performance of the PMF algorithm. We tested the two schemes suggested in Buchholz et al. (2020) with and without downweighing of low intensity signals. Assuming a Poisson-like distribution for the counting statistics of the mass spectrometer, the error values $S_{ij}(PL)$ were calculated with

$$100 \quad S_{ij}(PL) = a \cdot (X_{ij})^c + b \quad (\text{S4})$$

where X_{ij} is the signal intensity of the ion i at temperature/time j . a , b , and c are empirical parameters derived from the data set as described in (Buchholz et al., 2020). Here, their values are: $a = 0.62$, $b = 0.076$, and $c = 0.39$. For the constant error scheme (CN), which has a constant error value for one ion during one thermogram, the final 200 sec of the soak period was used to determine the noise value for each ion. The ion thermograms were smoothed with a Savitzky-Golay filter. The residual between these smoothed ion thermograms and the measured ion thermograms were calculated. The standard deviation of these residual for each ion is then set as the noise of this ion and used as its CN error value. For both error schemes, a minimum error value was applied. This was equal to the median of the CN error values (MinErr, 0.48 and 0.50 for α pin and SQTmix cases, respectively).

As both error schemes are not necessarily representing the “true” measurement error, the criteria $Q/Q_{exp} \rightarrow 1$ may not be satisfied. Apart from the overall change in Q/Q_{exp} , we also include the relative residual, how well peak shapes of ions are reproduced, and the overall interpretability of the factors as comprehensive measures of the quality of the PMF solution.

With the PL error scheme, the performance of the PMF algorithm was generally not satisfactory even with 12 factors. The PMF model underestimated the measured signals especially for the region around the T_{max} values of strong ions. Downweighing weak ions (signal to noise ratio < 2) did not improve this behavior. The unexplained variance could not be reduced below 10%. On the other hand, the CN error scheme yielded smaller overall residual values and unexplained variance values of $< 1\%$. The residuals

were distributed more evenly around 0 for each ion (i.e., no bias towards underestimation). For the CN error scheme, downweighing weak ions did not change the overall interpretation of the PMF factors. We thus decided to present the solution with the CN error and no downweighing in the manuscript.

S1.2.2 Selection of the optimal PMF solution

120 The most subjective part of PMF analysis is the selectin of the optimal solution, i.e., the number of factors. We carefully inspected solutions with up to 10 factors for α pin samples or 12 factors for SQTmix ones with multiple rotations. According to our evaluation criteria for the quality of the PMF solution, the eight-factor solution at $f_{\text{peak}} = 0$ was selected for the α pin SOA data set. In the same way, the ten-factor solution at $f_{\text{peak}} = -0.5$ was chosen for the SQTmix SOA data set, which yielded the most interpretable results. The PMF results are presented in Figure. S2 and S3. Note that compared to the α pin case, the two additional factors were
125 necessary to capture the more complex background in the SQTmix case. I.e., for SQTmix SOA data, the composition and signal strength of the background varied between experiment days, most likely due to some additional contamination of the setup caused by the necessary maintenance.

Figure S4 shows the Q/Q_{exp} vs number of factor curve for both data sets. The unscaled residuals, relative residuals, and scaled residuals of the 6-8 factor solution (8-10 factors, respectively) are depicted in Figure. S5 for both data sets. Already with six factors
130 for α pin SOA(or eight factors for SQTmix SOA, respectively), the residuals were in an acceptable range (relative residuals < 5% for most of the data set) and the change in Q/Q_{exp} was only gradual. However, increasing from six to seven factors for α pin SOA or eight to nine for SQTmix SOA improved the reconstruction of many ion peak shapes, especially for the high RH samples. This suggests that the additional factor enhanced the separation of the effect of isothermal evaporation from aqueous phase processes. With one more factor (eight and ten factors for α pin and SQTmix SOA), the aqueous phase processes became even more visible
135 in the factors. Thus, these solutions were selected for the detailed interpretation presented in the main manuscript. Increasing the number of factors further, either introduced more background factors or clearly splits one of the existing sample factors into two. The overall interpretation of the PMF solution would not be changed.

SI References

- 140 Buchholz, A., Ylisirniö, A., Huang, W., Mohr, C., Canagaratna, M., Worsnop, D. R., Schobesberger, S., and Virtanen, A.: Deconvolution of FIGAERO–CIMS thermal desorption profiles using positive matrix factorisation to identify chemical and physical processes during particle evaporation, *Atmos. Chem. Phys.*, 20, 7693-7716, 2020.
- Canagaratna, M. R., Jimenez, J. L., Kroll, J. H., Chen, Q., Kessler, S. H., Massoli, P., Hildebrandt Ruiz, L., Fortner, E., Williams, L. R., Wilson, K. R., Surratt, J. D., Donahue, N. M., Jayne, J. T., and Worsnop, D. R.: Elemental ratio measurements of organic compounds using aerosol mass spectrometry: Characterization, improved calibration, and implications, *Atmos. Chem. Phys.*, 15, 253-272, 2015.
- 145 Kang, E., Root, M. J., Toohey, D. W., and Brune, W. H.: Introducing the concept of potential aerosol mass (PAM), *Atmos. Chem. Phys.*, 7, 5727-5744, 2007.
- Kari, E., Miettinen, P., Yli-Pirila, P., Virtanen, A., and Faiola, C. L.: PTR-ToF-MS product ion distributions and humidity-dependence of biogenic volatile organic compounds, *Int. J. Mass Spectrom.*, 430, 87-97, 2018.
- 150 Lambe, A. T., Onasch, T. B., Massoli, P., Croasdale, D. R., Wright, J. P., Ahern, A. T., Williams, L. R., Worsnop, D. R., Brune, W. H., and Davidovits, P.: Laboratory studies of the chemical composition and cloud condensation nuclei (CCN) activity of secondary organic aerosol (SOA) and oxidized primary organic aerosol (OPOA), *Atmos. Chem. Phys.*, 11, 8913-8928, 2011.
- Lopez-Hilfiker, F. D., Mohr, C., Ehn, M., Rubach, F., Kleist, E., Wildt, J., Mentel, T. F., Lutz, A., Hallquist, M., Worsnop, D., and Thornton, J. A.: A novel method for online analysis of gas and particle composition: Description and evaluation of a filter inlet for gases and aerosols (FIGAERO), *Atmos. Meas. Tech.*, 7, 983-1001, 2014.
- 155 Paatero, P. and Tapper, U.: Positive matrix factorization: A non-negative factor model with optimal utilization of error estimates of data values, *Environmetrics*, 5, 111-126, 1994.
- Peng, Z., Day, D. A., Ortega, A. M., Palm, B. B., Hu, W. W., Stark, H., Li, R., Tsigaridis, K., Brune, W. H., and Jimenez, J. L.: Non-OH chemistry in oxidation flow reactors for the study of atmospheric chemistry systematically examined by modeling, *Atmos. Chem. Phys.*, 16, 4283-4305, 2016.
- 160 Peng, Z., Day, D. A., Stark, H., Li, R., Lee-Taylor, J., Palm, B. B., Brune, W. H., and Jimenez, J. L.: Hox radical chemistry in oxidation flow reactors with low-pressure mercury lamps systematically examined by modeling, *Atmos. Meas. Tech.*, 8, 4863-4890, 2015.
- Ulbrich, I. M., Canagaratna, M. R., Zhang, Q., Worsnop, D. R., and Jimenez, J. L.: Interpretation of organic components from positive matrix factorization of aerosol mass spectrometric data, *Atmos. Chem. Phys.*, 9, 2891-2918, 2009.
- 165 Ylisirniö, A., Barreira, L. M. F., Pullinen, I., Buchholz, A., Jayne, J., Krechmer, J. E., Worsnop, D. R., Virtanen, A., and Schobesberger, S.: On the calibration of FIGAERO-tof-CIMS: Importance and impact of calibrant delivery for the particle-phase calibration, *Atmos. Meas. Tech.*, 14, 355-367, 2021.

170 **Table S1.** Experimental Conditions and Results for Biogenic SOA Generated from the OFR

	α -pinene	sesquiterpene mixture
abbreviation	α pin	SQTmix
[VOC] _{OFR} (ppb) ^a	254 ± 11	261 ± 5
[O ₃] _{OFR} (ppm) ^b	9.76 ± 0.31	9.55 ± 0.37
T _{OFR} (°C)	24.6 ± 0.9	25.50 ± 0.81
RH _{OFR} (%)	44.4 ± 2.3	40.86 ± 0.99
residence time (s)	160	161
effective OH exposure (10 ¹¹ molec cm ⁻³) ^c	2.6 ± 0.3	0.9 ± 0.1
oxygen-to-carbon (O:C) ^d	0.77 ± 0.03	0.95 ± 0.06
oxidation state (OSc) ^d	0.05 ± 0.04	0.50 ± 0.17

^aMixing ratio of VOC was corrected with the dilution of O₃-contained flow but without the loss due to pure ozonolysis at the inlet.

^bO₃ was measured at the OFR outlet after 254-nm UV lamps were switched on but without the addition of VOC precursors. ^cOH exposure was calculated with the OFR model (Peng et al., 2015; Peng et al., 2016) by taking the external OH reactivity into account.

^dThe values of the oxygen to carbon ratio (O:C) and the oxidation state (OSc) were derived from the HR-ToF-AMS measurement data of monodisperse SOA particles which represents the particle population used for isothermal evaporation measurements.

175

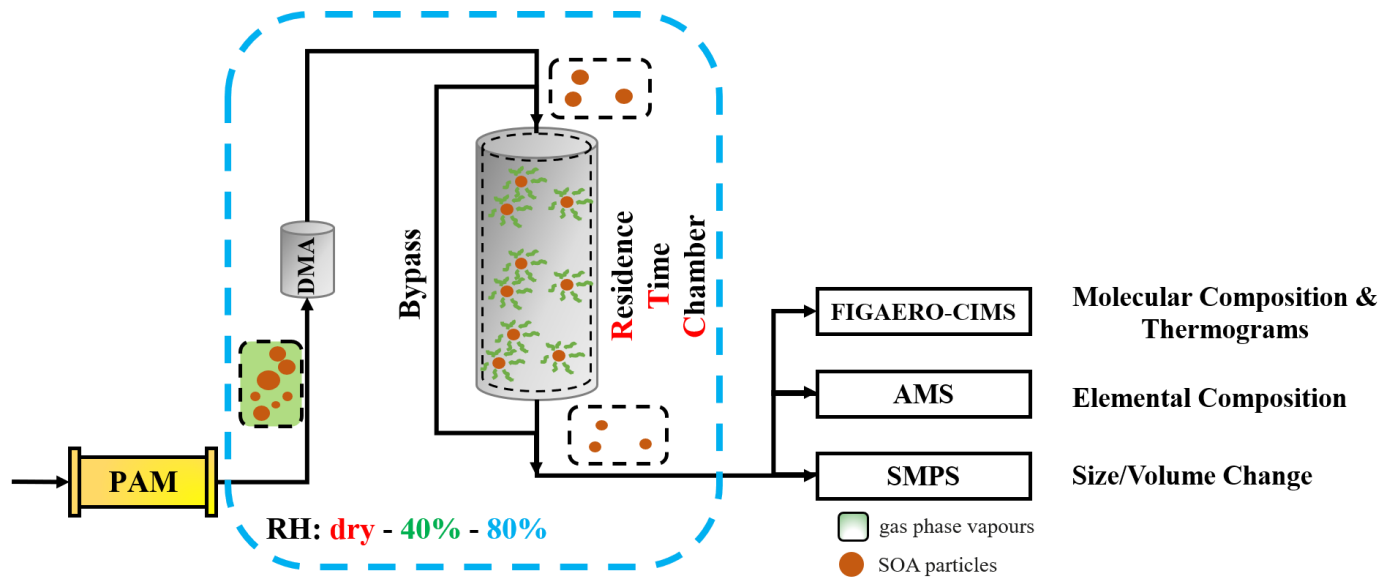


Figure S1. Experimental setup for evaporation experiments of α -pinene and sesquiterpene-mixed SOA particles. Parts in the blue-dashed area were regulated with active humidity control.

180

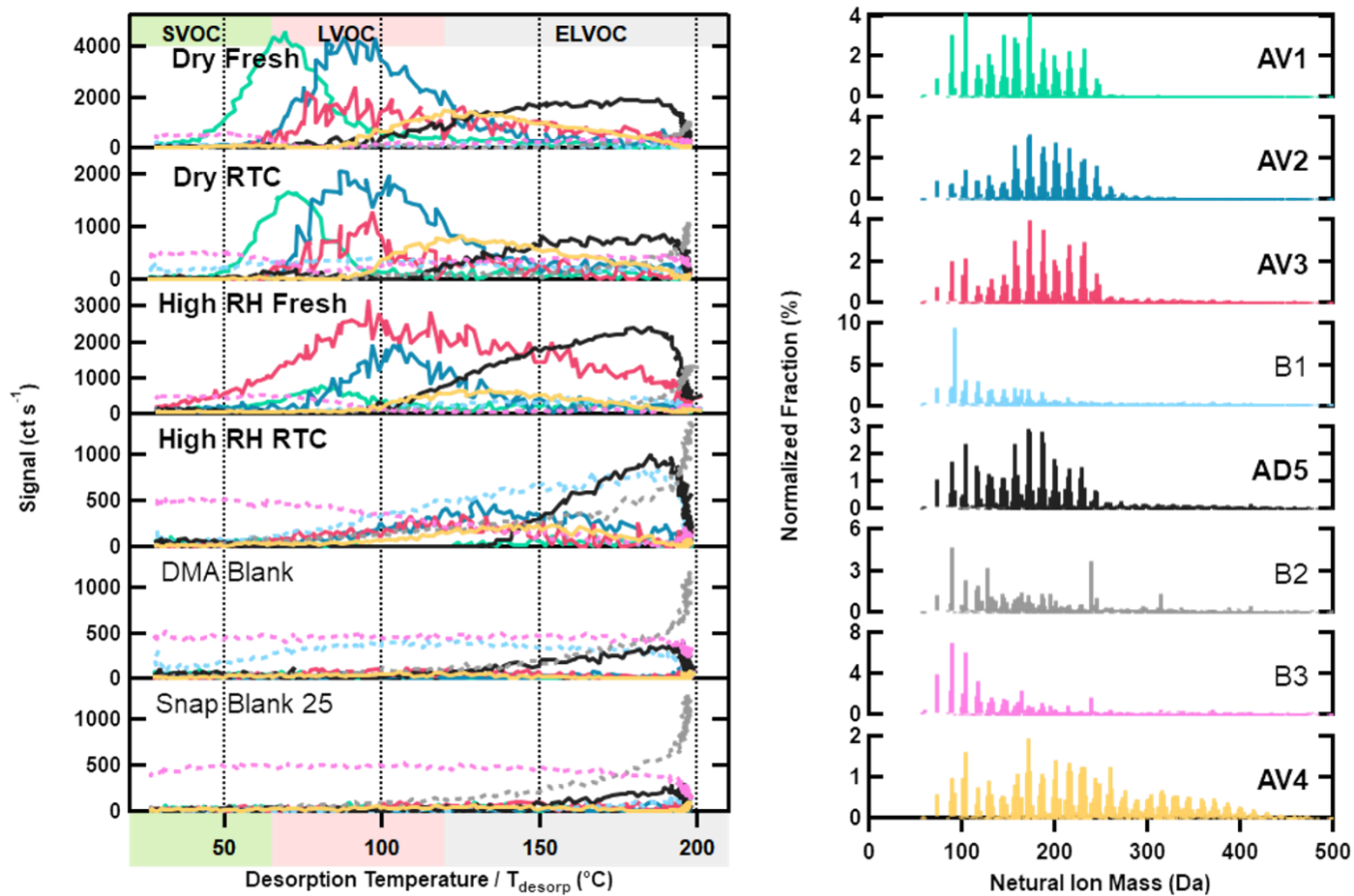


Figure S2. Sample (solid lines) and background (dashed lines) factors from an eight-factor PMF solution for α pin SOA particles. Factor thermograms are shown with color bands indicating volatility categorization on the left panel, while normalized factor mass spectrums are presented on the right panel. The color code is identical for both panels.

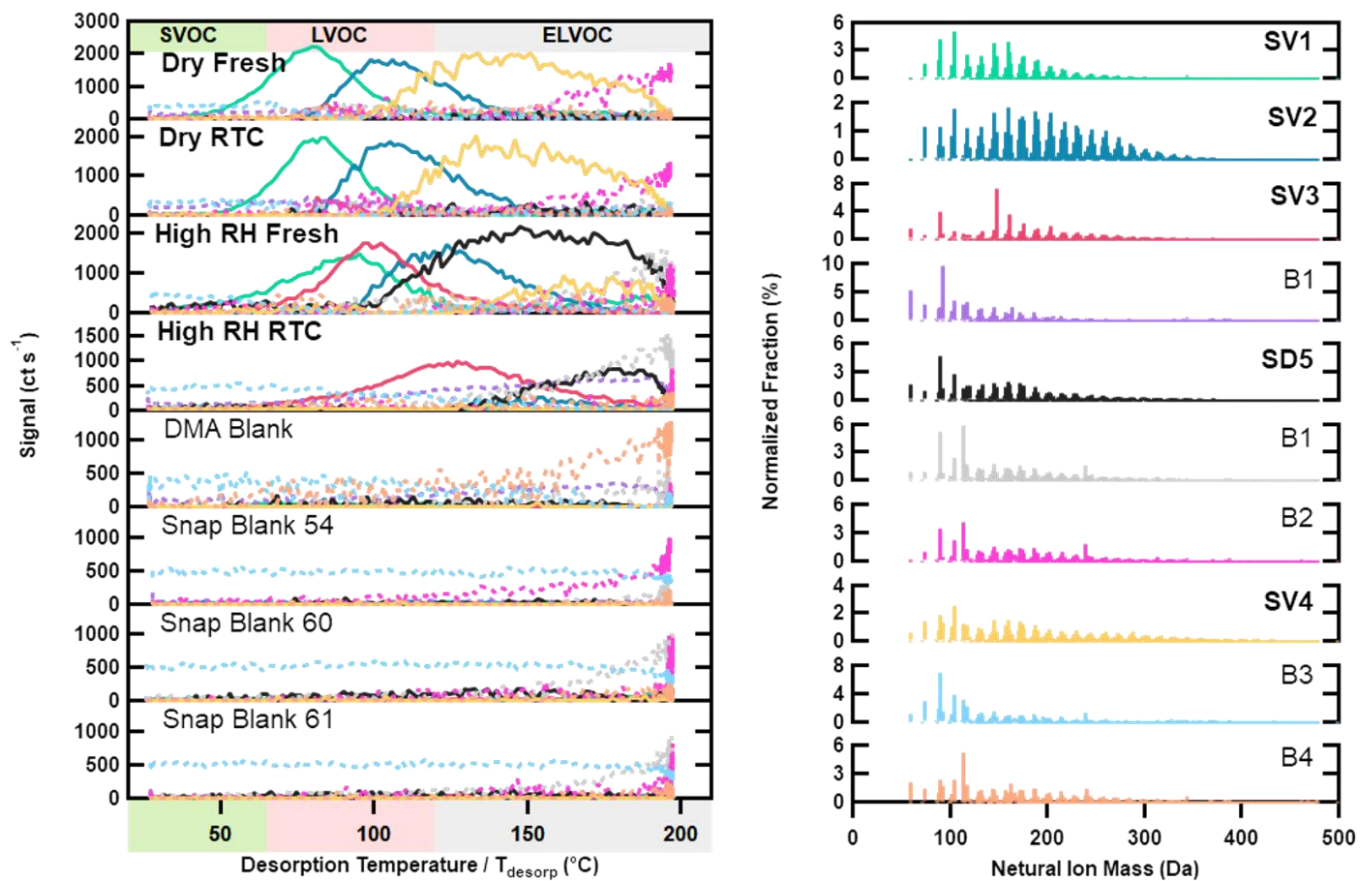


Figure S3. Sample (solid lines) and background (dashed lines) factors from a ten-factor PMF solution for SQTmix SOA particles. Factor thermograms are shown with color bands indicating volatility categorization on the left panel, while normalized factor mass spectrums are presented on the right panel. The color code is identical for both panels.

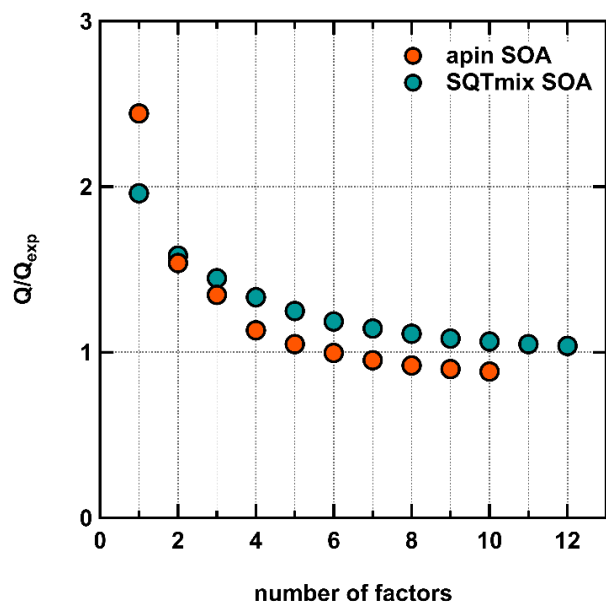
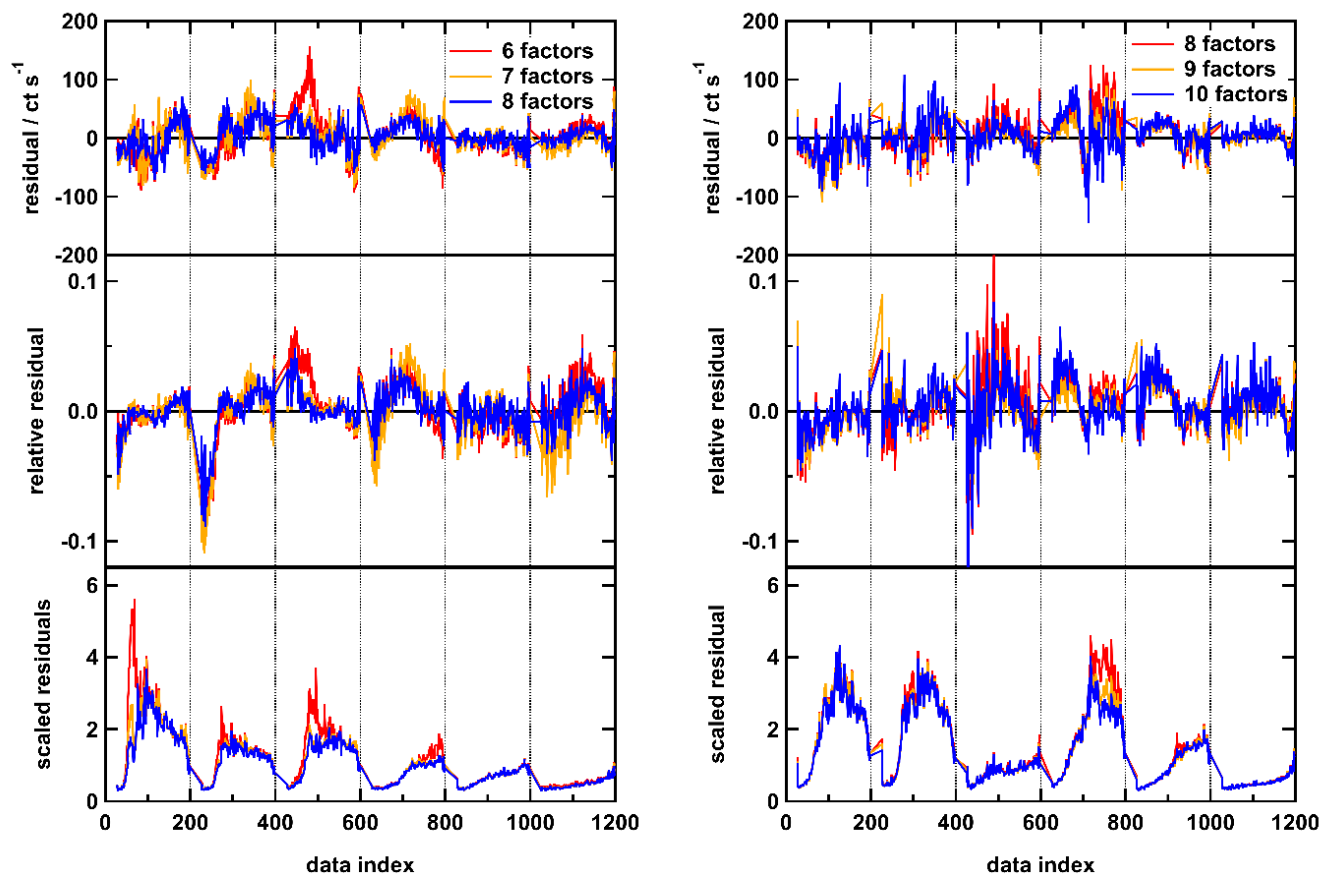
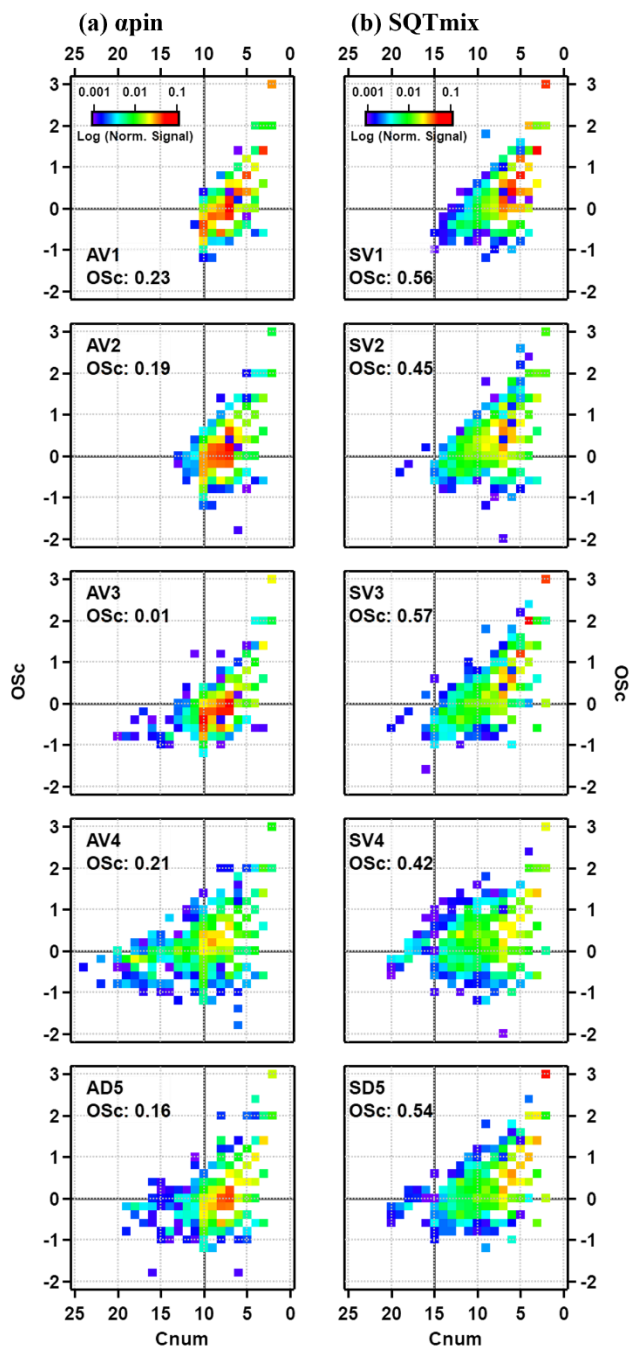


Figure S4. Q/Q_{exp} values for PMF solutions for α pin (orange) and SQTmix (turquoise) SOA data sets.



195 **Figure S5.** “Time” series of residuals, relative residuals, and scaled residuals for the 6 – 8 factor solutions for the α pin SOA data set (left) and the 8 – 10 factor solutions of the SQTmix SOA data set (right). The four samples and two blanks are plotted vs a data index which is $T_{\text{desorp}} + (i \cdot 200 \text{ } ^\circ\text{C})$. Vertical dashed lines indicate the start of the next sample. The order is: fresh, dry (0-200); RTC,dry (200-400); fresh, high RH (400-600); RTC, high RH (600-800); DMA blank (800-1000); snap blank (1000-1200).



200 **Figure S6.** Kroll diagrams for main sample factors in α pin (a) and SQTmix (b) SOA particles. For a set of organic compounds containing the same number of carbon atoms, they are grouped into cells with intervals of 0.2 in carbon oxidation state (Osc). Each cell is colored-coded by the logarithm of the total sum of normalized signals. While solid horizontal lines mark the Osc values of 0, solid vertical ones indicate the carbon numbers of the respective SOA precursors.